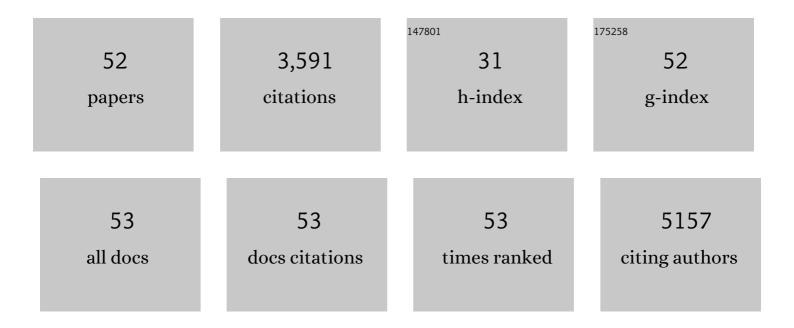
Soonhyun Kim

List of Publications by Year in descending order

Source: https://exaly.com/author-pdf/785507/publications.pdf Version: 2024-02-01



#	Article	IF	CITATIONS
1	Visible Light Active Platinum-Ion-Doped TiO2Photocatalyst. Journal of Physical Chemistry B, 2005, 109, 24260-24267.	2.6	384
2	Photocatalytic Comparison of TiO ₂ Nanoparticles and Electrospun TiO ₂ Nanofibers: Effects of Mesoporosity and Interparticle Charge Transfer. Journal of Physical Chemistry C, 2010, 114, 16475-16480.	3.1	330
3	Kinetics and Mechanisms of Photocatalytic Degradation of (CH3)nNH4-n+(0 ≤≤4) in TiO2Suspension:Â The Role of OH Radicals. Environmental Science & Technology, 2002, 36, 2019-2025.	10.0	264
4	Visible-Light-Induced Photocatalytic Degradation of 4-Chlorophenol and Phenolic Compounds in Aqueous Suspension of Pure Titania:  Demonstrating the Existence of a Surface-Complex-Mediated Path. Journal of Physical Chemistry B, 2005, 109, 5143-5149.	2.6	252
5	Preparation of mesoporous In2O3 nanofibers by electrospinning and their application as a CO gas sensor. Sensors and Actuators B: Chemical, 2010, 149, 28-33.	7.8	195
6	Effects of surface fluorination of TiO2 on the photocatalytic degradation of tetramethylammonium. Journal of Photochemistry and Photobiology A: Chemistry, 2003, 160, 55-60.	3.9	160
7	Heterogeneous photocatalytic treatment of pharmaceutical micropollutants: Effects of wastewater effluent matrix and catalyst modifications. Applied Catalysis B: Environmental, 2014, 147, 8-16.	20.2	130
8	Comparative Study of Homogeneous and Heterogeneous Photocatalytic Redox Reactions:Â PW12O403-vs TiO2. Journal of Physical Chemistry B, 2004, 108, 6402-6411.	2.6	120
9	Dual Photocatalytic Pathways of Trichloroacetate Degradation on TiO2:  Effects of Nanosized Platinum Deposits on Kinetics and Mechanism. Journal of Physical Chemistry B, 2002, 106, 13311-13317.	2.6	119
10	Boosting the electrocatalytic activities of SnO2 electrodes for remediation of aqueous pollutants by doping with various metals. Applied Catalysis B: Environmental, 2012, 111-112, 317-325.	20.2	111
11	Preparation of TiO2-embedded carbon nanofibers and their photocatalytic activity in the oxidation of gaseous acetaldehyde. Applied Catalysis B: Environmental, 2008, 84, 16-20.	20.2	92
12	Effects of electrolyte on the electrocatalytic activities of RuO2/Ti and Sb–SnO2/Ti anodes for water treatment. Applied Catalysis B: Environmental, 2010, 97, 135-141.	20.2	86
13	Efficient visible light-induced H2 production by Au@CdS/TiO2 nanofibers: Synergistic effect of core–shell structured Au@CdS and densely packed TiO2 nanoparticles. Applied Catalysis B: Environmental, 2015, 166-167, 423-431.	20.2	83
14	Graphene oxide embedded into TiO2 nanofiber: Effective hybrid photocatalyst for solar conversion. Journal of Catalysis, 2014, 309, 49-57.	6.2	77
15	Rapid removal of radioactive cesium by polyacrylonitrile nanofibers containing Prussian blue. Journal of Hazardous Materials, 2018, 347, 106-113.	12.4	77
16	Preparation of ZnO nanorods by microemulsion synthesis and their application as a CO gas sensor. Sensors and Actuators B: Chemical, 2011, 160, 94-98.	7.8	75
17	Simultaneous conversion of dye and hexavalent chromium in visible light-illuminated aqueous solution of polyoxometalate as an electron transfer catalyst. Applied Catalysis B: Environmental, 2008, 84, 148-155.	20.2	69
18	Accelerated photocatalytic degradation of organic pollutants over carbonate-rich lanthanum-substituted zinc spinel ferrite assembled reduced graphene oxide by ultraviolet (UV)-activated persulfate. Chemical Engineering Journal, 2020, 393, 124733.	12.7	67

SOONHYUN KIM

#	Article	IF	CITATIONS
19	Electrochemically deposited Fe2O3 nanorods on carbon nanofibers for free-standing anodes of lithium-ion batteries. Carbon, 2015, 94, 9-17.	10.3	66
20	Synthesis of Al-doped ZnO Nanorods via Microemulsion Method and Their Application as a CO Gas Sensor. Journal of Materials Science and Technology, 2015, 31, 639-644.	10.7	65
21	Enhancement of photocatalytic activity of titania–titanate nanotubes by surface modification. Applied Catalysis B: Environmental, 2012, 123-124, 391-397.	20.2	49
22	Titania nanofibers as a photo-antenna for dye-sensitized solar hydrogen. Photochemical and Photobiological Sciences, 2012, 11, 1437-1444.	2.9	40
23	High performance catalyst for electrochemical hydrogen evolution reaction based on SiO2/WO3â^' nanofacets. International Journal of Hydrogen Energy, 2013, 38, 9732-9740.	7.1	40
24	Sequential removal of radioactive Cs by electrochemical adsorption and desorption reaction using core-shell structured carbon nanofiber–Prussian blue composites. Chemical Engineering Journal, 2020, 399, 125817.	12.7	40
25	Core–shell-structured carbon nanofiber-titanate nanotubes with enhanced photocatalytic activity. Applied Catalysis B: Environmental, 2014, 148-149, 170-176.	20.2	38
26	Carbon nanotubes as an auxiliary catalyst in heterojunction photocatalysis for solar hydrogen. Applied Catalysis B: Environmental, 2013, 142-143, 647-653.	20.2	35
27	Synthesis and characterization of platinum modified TiO ₂ -embedded carbon nanofibers for solar hydrogen generation. RSC Advances, 2014, 4, 51286-51293.	3.6	35
28	Electrocatalytic activities of Sb-SnO2 and Bi-TiO2 anodes for water treatment: Effects of electrocatalyst composition and electrolyte. Catalysis Today, 2017, 282, 57-64.	4.4	35
29	Visible light-induced photocatalytic oxidation of 4-chlorophenol and dichloroacetate in nitrided Pt-TiO2 aqueous suspensions. Journal of Photochemistry and Photobiology A: Chemistry, 2009, 203, 145-150.	3.9	34
30	Prussian blue-embedded carboxymethyl cellulose nanofibril membranes for removing radioactive cesium from aqueous solution. Carbohydrate Polymers, 2020, 235, 115984.	10.2	33
31	Self-assembled TiO2 agglomerates hybridized with reduced-graphene oxide: A high-performance hybrid photocatalyst for solar energy conversion. Chemical Engineering Journal, 2015, 262, 409-416.	12.7	32
32	Trilayer CdS/carbon nanofiber (CNF) mat/Pt-TiO2 composite structures for solar hydrogen production: Effects of CNF mat thickness. Applied Catalysis B: Environmental, 2016, 196, 216-222.	20.2	32
33	Homogeneous photoconversion of seawater uranium using copper and iron mixed-oxide semiconductor electrodes. Applied Catalysis B: Environmental, 2017, 207, 35-41.	20.2	27
34	Simultaneous removal of radioactive cesium and strontium from seawater using a highly efficient Prussian blue-embedded alginate aerogel. Journal of Environmental Management, 2021, 297, 113389.	7.8	27
35	CdS-loaded flexible carbon nanofiber mats as a platform for solar hydrogen production. International Journal of Hydrogen Energy, 2015, 40, 136-145.	7.1	25
36	ZnO nanostructure electrodeposited on flexible conductive fabric: A flexible photo-sensor. Sensors and Actuators B: Chemical, 2017, 240, 1106-1113.	7.8	25

SOONHYUN KIM

#	Article	IF	CITATIONS
37	Photocatalytic enhancement of cesium removal by Prussian blue-deposited TiO2. Journal of Hazardous Materials, 2018, 357, 449-456.	12.4	23
38	Conventional and photoinduced radioactive 137Cs removal by adsorption on FeFe, CoFe, and NiFe Prussian blue analogues. Chemical Engineering Journal, 2021, 405, 126568.	12.7	23
39	Decrease of Reactive Oxygen Species-Related Biomarkers in the Tissue-Mimic 3D Spheroid Culture of Human Lung Cells Exposed to Zinc Oxide Nanoparticles. Journal of Nanoscience and Nanotechnology, 2014, 14, 3356-3365.	0.9	22
40	Ambient-temperature catalytic degradation of aromatic compounds on iron oxide nanorods supported on carbon nanofiber sheet. Applied Catalysis B: Environmental, 2019, 259, 118066.	20.2	21
41	Characterization of Ga-doped ZnO Nanorods Synthesized via Microemulsion Method. Journal of Materials Science and Technology, 2013, 29, 39-43.	10.7	18
42	Photocatalytic reactivity and diffusing OH radicals in the reaction medium containing TiO2 particles. Korean Journal of Chemical Engineering, 2001, 18, 898-902.	2.7	16
43	Titania-coated plastic optical fiber fabrics for remote photocatalytic degradation of aqueous pollutants. Journal of Environmental Chemical Engineering, 2017, 5, 1899-1905.	6.7	16
44	Effects of ion exchange and calcinations on the structure and photocatalytic activity of hydrothermally prepared titanate nanotubes. Crystal Research and Technology, 2012, 47, 1190-1194.	1.3	15
45	Effects of hydrothermal temperature and acid concentration on the transition from titanate to titania. Journal of Industrial and Engineering Chemistry, 2012, 18, 1141-1148.	5.8	15
46	Visible light-induced photocatalytic degradation of gas-phase acetaldehyde with platinum/reduced titanium oxide-loaded carbon paper. RSC Advances, 2017, 7, 50693-50700.	3.6	12
47	Effect of ZnO Electrodeposited on Carbon Film and Decorated with Metal Nanoparticles for Solar Hydrogen Production. Journal of Materials Science and Technology, 2016, 32, 1059-1065.	10.7	11
48	Enhancement of cesium adsorption on Prussian blue by TiO2 photocatalysis: Effect of the TiO2/PB ratio. Journal of Water Process Engineering, 2020, 38, 101571.	5.6	8
49	Metal nanoparticles decorated PET/PET-TiO2 bi-component filaments by photocatalytic deposition. Textile Reseach Journal, 2012, 82, 1973-1981.	2.2	7
50	<i>In vivo</i> removal of radioactive cesium compound using Prussian blue-deposited iron oxide nanoparticles. Nanomedicine, 2019, 14, 3143-3158.	3.3	7
51	Photoreaction characteristics of ferrous oxalate recovered from wastewater. Chemosphere, 2020, 249, 126201.	8.2	7
52	Fe2O3 nanorods on carbon nanofibers induce spontaneous reductive transformation of inorganic contaminants in ambient aerated water. Chemical Engineering Journal, 2022, 429, 132108.	12.7	1